buildings

MDPI

Article

Research on the Characteristics and Comprehensive Mitigation Measures of Vibration and Acoustic Environment in Building Clusters Above Metro Depots

Jian Li [1], Xiaohong Xue [1], Jian Wang [1], Wanliang Kang [1], Boyang Zhang [1], Zhengye Huang [1], Yuan Mei [2] and Xin Ke [2,*]

[1] China Railway 20th Bureau Group Sixth Engineering Co., Ltd., Xi'an 710032, China; lijian.20g@crcc.cn (J.L.); xuexiaohong.20g@crcc.cn (X.X.); jianwangzgzt@163.com (J.W.); wanoliangkangzgzt@163.com (W.K.); boyangzhangzgzt@163.com (B.Z.); zichen1635743808@163.com (Z.H.)

[2] School of Civil Engineering, Xi'an University of Architecture and Technology, Xi'an 710055, China; meiyuan@xauat.edu.cn

* Correspondence: kx20220408@xauat.edu.cn

Abstract

Taking a metro over-track TOD (Transit-Oriented Development) project in Chongqing as the engineering background, this study adopts a combined research approach integrating field measurements and numerical simulation. A coupled finite element model of the train–track–tunnel–soil–building system and a regional acoustic model are established to systematically reveal the vibration response characteristics of building clusters above the depot induced by metro operation, the propagation mechanism of structure-borne secondary noise, and the distribution patterns of the regional acoustic environment, while identifying the areas where vibration and noise exceed the prescribed limits as well as the key influencing factors. On this basis, following a hierarchical mitigation strategy consisting of source control, path interruption, and receiver protection, an integrated control scheme is proposed through the coordinated application of track vibration reduction, building vibration isolation, acoustic environment optimization, and building sound insulation. The engineering applicability and control effectiveness of the proposed scheme are further verified by numerical simulation. The findings of this study can provide theoretical support and technical reference for the refined design and integrated prevention and control of vibration and acoustic environments in similar metro over-track development projects.

Keywords: metro over-track development; TOD building clusters; vibration characteristics; secondary noise; acoustic environment evaluation; integrated mitigation measures

Check for updates

Academic Editor: Ángel Fermín Ramos Ridao

Received: 15 March 2026
Revised: 20 April 2026
Accepted: 22 April 2026
Published: 30 April 2026

Copyright: © 2026 by the authors. Licensee MDPI, Basel, Switzerland. This article is an open access article distributed under the terms and conditions of the Creative Commons Attribution (CC BY) license.

1. Introduction

The transit-oriented development (TOD) model enables the optimization of rail transit vehicle depot construction and related land resources. Guided by the TOD concept, the commercial facilities in depot overbuilds evolve from early-stage community service-oriented commerce to multi-level commercial developments integrated with the urban context through close linkage with public transit. In recent years, overbuild projects above vehicle depots have become a typical model in urban rail development, playing an important role in promoting regional coordinated development and recouping investments in metro construction [1–4]. However, the construction and operation of the metro bring a series of challenges: during train operation, the interaction between wheels and rails

generates vibrations that propagate as vibrational waves to the overlying and surrounding buildings, causing structural vibrations and inducing secondary structure-borne noise, which seriously affects people's daily life and work quality [5–7], and in severe cases, may pose risks to human health. At the same time, TOD projects are often located at major public transportation nodes, where high traffic volumes generate complex noise, further exacerbating the deterioration of the regional acoustic environment [8–10].

The impact of vibration and noise on civil engineering structures and their service performance has become a common research topic in the fields of civil and environmental engineering, with implications spanning virtually all building types and the entire engineering lifecycle [11]. Multi-source dynamic excitations, including road traffic loads, rail transit operation, industrial equipment operation, and civil engineering construction activities, can all induce dynamic responses of the site and building structures, as well as secondary noise radiation. For civil buildings such as residential, commercial, and office buildings, the primary concern lies in their influence on indoor environmental comfort and user experience [12,13]. For special buildings such as high-precision research facilities, laboratories for precision instruments, and semiconductor manufacturing workshops, however, the sensitivity to ground microvibration and environmental noise is extremely high. Even nanometer-scale vibration displacement may lead to a decline in equipment accuracy, distortion of experimental data, or even system failure [14]. Relevant engineering practice has already carried out source intensity measurements and long-term monitoring of ground-motion conditions during construction for the High-Luminosity Large Hadron Collider upgrade project, thereby establishing quantitative criteria for microvibration control. Owing to the significant differences in spectral characteristics, propagation patterns, and action intensities among different vibration sources, the vibration and noise effects under multi-source coupling are considerably more complex and may produce differentiated impacts on buildings with different structural forms and functional purposes [15].

Scholars both domestically and internationally have conducted extensive research on vibrations and secondary noise induced by metro operation. In terms of the mechanism of vibration propagation, studies have shown that irregularities among train wheels, rails, and track structures increase vibration intensity during operation, and the vehicle-induced vibration source exhibits characteristics of mobility and intermittency [16,17]. The impact of vehicle-induced vibration on adjacent buildings is related to factors such as building height and structural system, and the vertical vibration response is significantly greater than the horizontal vibration response. In terms of prediction methods, some scholars have employed two-dimensional finite element methods to predict ground vibrations generated by underground train operation, finding that when the distance from the tunnel exceeds 50 m, the vibration reduction form of the track has little influence on ground vibration; other scholars have adopted three-dimensional finite element methods to investigate the vibration effects caused by overlapping stations and train operations [18,19]. In recent years, the FE–SEA hybrid method has been applied to the broadband vibration and noise analysis of overbuild structures. Studies have shown that the dominant vibration frequencies of floor slabs in overbuild structures are mainly located in the low-frequency range of 31.5–50 Hz, and the sound pressure of secondary structure-borne noise in typical rooms is primarily concentrated within the 20–80 Hz range. In the field of acoustic environment research, scholars both domestically and internationally have systematically analyzed the spatiotemporal distribution, statistical characteristics, and influencing factors of road traffic noise, revealing that vehicle speed, traffic volume, and vehicle type proportion are the primary factors affecting road traffic noise. Environmental noise tests of metro viaduct lines have also shown that strong structural noise is mainly concentrated in the mid-span region of bridges [20–22]. In response to problems induced by metro operation, scholars

both domestically and internationally have conducted related studies from the perspective of vibration and noise reduction. The floating slab track bed has been shown to provide significant vibration mitigation effects; the effectiveness of vibration isolation measures such as isolation trenches, infilled trenches, and wave barriers has been comparatively analyzed; structural vibration isolation measures, including spring isolation bearings and tuned mass dampers (TMDs), have been demonstrated to achieve good vibration reduction performance; and the height and distance of noise barriers, as well as the installation of sound-absorbing materials, have been found to significantly influence the effectiveness of noise reduction [23,24].

Although the aforementioned studies have been conducted, systematic and comprehensive investigations on the vibration characteristics of metro overbuild building clusters, the propagation mechanisms of secondary noise, and the spatial distribution characteristics of the acoustic environment under the TOD model remain relatively limited. In particular, studies that simultaneously consider structure-borne vibrations induced by metro operation and the regional acoustic environment dominated by road traffic, while proposing integrated mitigation measures, are still scarce.

To address this issue, the present study takes a TOD project in Chongqing as the engineering background and adopts a combined approach of field measurements and numerical simulation. A coupled analytical framework integrating a three-dimensional finite element model of the train–track–tunnel–soil–building system with a regional acoustic model is established, thereby enabling the synchronous simulation and combined assessment of metro-induced structural vibration, structure-borne secondary noise, and road traffic noise. On this basis, the vibration response characteristics and secondary noise propagation patterns of building clusters in different functional zones, including residential, office, rental housing, and reserved areas, are systematically analyzed, and the combined influence mechanism of road traffic and rail transit on the regional acoustic environment is further investigated. In addition, an integrated mitigation strategy is proposed, covering track vibration reduction, building vibration isolation, propagation path interruption, and receiver protection, and its effectiveness in controlling vibration and noise is verified through numerical simulation. The findings of this study are expected to provide a useful reference for the integrated control of vibration and acoustic environments in similar TOD projects.

2. Engineering Overview and Research Methodology

2.1. Engineering Overview

This study takes the TOD project located in the Nanping cluster, Nan'an District, Chongqing, as the research object. The project is situated on the depot site of the Chongqing Rail Transit Loop Line Sili Gongli Parking Yard, representing a typical over-track comprehensive development project under the Transit-Oriented Development (TOD) model. The project aims to realize property development above the pile foundation system of the metro depot, thereby achieving efficient utilization of land resources, promoting coordinated regional development, and simultaneously providing financial support for rail transit construction investment.

The Sili Gongli Parking Yard is an important component of the Chongqing Rail Transit Loop Line, undertaking functions such as train operation, servicing and preparation, maintenance, and vehicle stabling. The Loop Line has a total length of approximately 50.88 km and serves as a backbone line of Chongqing's urban rail transit network, as well as the only fully closed-loop line in the system. It passes through several key commercial and residential areas, including Chongqing Library, Sili Gongli, and Erlang. The parking yard site extends approximately 750 m in the north–south direction and 190 m in the east–west direction. The eastern side is adjacent to Haixia Road, a major urban arterial road, while the

western side is close to Zong'er Road, a secondary urban road. The southern side borders the Sili Gongli transfer hub, making the site of significant transportation importance. The location of the project is shown in Figure 1.

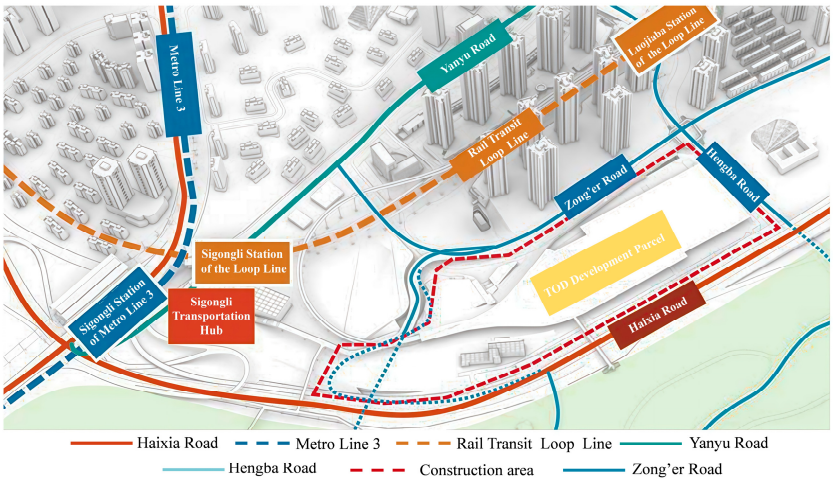


Figure 1. Plan View of Road Distribution Surrounding the Project.

The total development area of the project is approximately 161,400 m^2. An over-track comprehensive development scheme is adopted, in which property development is constructed above the metro parking yard. According to functional zoning, the project mainly consists of a high-rise residential area, a rental housing area, an office area, and a reserved area. Among them, the residential area comprises 13 high-rise buildings, the rental housing area corresponds to Building No. 16, and the office area corresponds to Building No. 17. The reserved area includes Buildings No. 14 and No. 15. The delineation of these functional zones not only serves different usage requirements but also provides a basis for the subsequent zonal evaluation of vibration and noise characteristics, as shown in Figure 2.

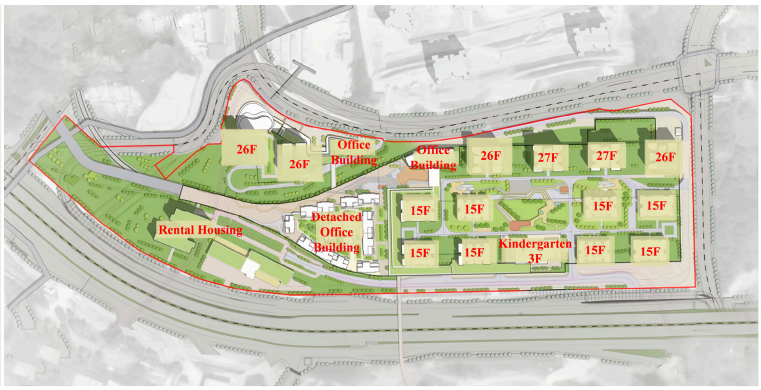


Figure 2. Plan View of Building Distribution of the Project.

The project is surrounded by a dense transportation network, resulting in complex noise sources. In addition to the rail transit Loop Line, the project site is located adjacent to Haixia Road and Zong'er Road, which are urban arterial and secondary roads with large traffic volumes and relatively high vehicle speeds, making them the primary contributors to the regional acoustic environment. Rail transit lines run around the perimeter of the site. The operating speed of trains is approximately 15 km/h in the throat (switching) area and about 5 km/h within the depot area. During operation, the vibration and the associated structure-borne secondary noise generated by train movement have a significant impact on the building clusters above the site.

According to the results of the site geotechnical investigation, the strata in the project area from top to bottom consist of plain fill, strongly weathered sandy mudstone, and moderately weathered sandy mudstone. The physical and mechanical parameters of each layer are presented in Table 1. These geological conditions provide the fundamental data for subsequent finite element modeling and vibration propagation analysis.

Table 1. Physical and Mechanical Properties of Soil and Rock Strata.

Depth/(m)	Soil Properties	Unit Weight/(kN/m^3)	Elastic Modulus/(MPa)	Poisson's Ratio
0~10	Plain Fill	18.0	45	0.4
10~11.2	Strongly Weathered Sandy Mudstone	24.6	367	0.3
below 11.2 m	Moderately Weathered Sandy Mudstone	25.6	1750	0.2

2.2. Overview of Research Methodology

This study adopts a combined approach of field measurements and numerical simulation. Vibration and noise monitoring points were deployed at the site of a TOD project in Chongqing to collect measured data under the influence of metro operation and road traffic, providing a basis for model construction and parameter calibration. Based on these measurements, two types of numerical simulation models were established. First, a 3D finite element model of train–track–tunnel–soil–building was developed based on the vehicle–track coupled dynamics theory to simulate the structural vibration response induced by metro operation. The secondary structure-borne noise was then calculated according to the JGJ/T 170-2009 standard [25]. Second, a regional acoustic model was constructed using Cadna/A software, with inputs including road traffic flow and rail transit noise source intensity, to predict noise distribution under three scenarios: road traffic only, rail transit only, and the combined effect of both sources. The measured vibration acceleration, Z-weighted vibration level, and equivalent noise level were compared with the simulation results. Key parameters were adjusted to ensure that the dominant vibration frequencies matched and that the noise error remained within 1.1 dB. Furthermore, targeted vibration mitigation and noise reduction measures were designed for areas exceeding standard limits. The validated models were then used to evaluate the response indicators after implementation, analyze the control effectiveness, and propose optimization recommendations.

3. Characteristics of Environmental Vibration and Propagation Patterns of Secondary Noise

3.1. Establishment of the Vibration Characteristics Model

In this project, the general-purpose finite element software ABAQUS 2021 was adopted to establish a finite element (FE) model of the coupled soil–track–building system. The model was built at a 1:1 scale according to the design drawings and actual site conditions, incorporating detailed representations of the structural layers of the Chongqing Rail Transit Loop Line parking yard, the overlying buildings, and the track, thereby enabling simulation of the vibration response of different buildings as trains pass at varying speeds. The soil strata were divided into three layers based on geotechnical survey results, with parameters adopted from Table 1. The train model consisted of a 6-car As-type train operating at 15 km/h in the throat area and 5 km/h in the depot area, with detailed parameters listed in Table 2. The track is a conventional ballasted track, with parameters provided in Table 3. To more effectively excite soil vibrations, track irregularities were modeled by superimposing the U.S. five-level spectrum and Sato short-wave irregularities [26]. Additionally, to eliminate the influence of boundary-reflected waves, the model simulates the semi-infinite soil domain beyond the FE model by extending a layer of identical elements along the normals

at the established boundaries, representing the surrounding semi-infinite soil outside the modeled region [27].

Table 2. Train Modeling Parameters.

Name	Unit	Value
Car body mass M_c	kg	41,610
Frame mass M_t	kg	4280
Wheelset mass M_w	kg	1860
Vehicle length	m	22.8
Vehicle spacing l_c	m	15.7
Bogie wheelbase l_t	m	2.5
Wheel rolling circle radius R	m	0.42

Table 3. Track Modeling Parameters.

Name	Unit	Value
Rail elastic modulus E	N/m^2	2.06×10^{11}
Rail cross-sectional moment of inertia I	m^4	3.22×10^{-5}
Unit length mass of rail m_r	kg/m	60.64
Fastener spacing l_s	m	0.6
Rail pad stiffness k_p	N/m	4×10^7
Rail pad damping C_p	N/m	3×10^4

Based on the above description, the model contains a total of 6.125×10^6 elements and 6.234×10^6 nodes, with an element length of 0.5 m and a time integration step of 2 ms. The finite element simulation model is shown in Figure 3.

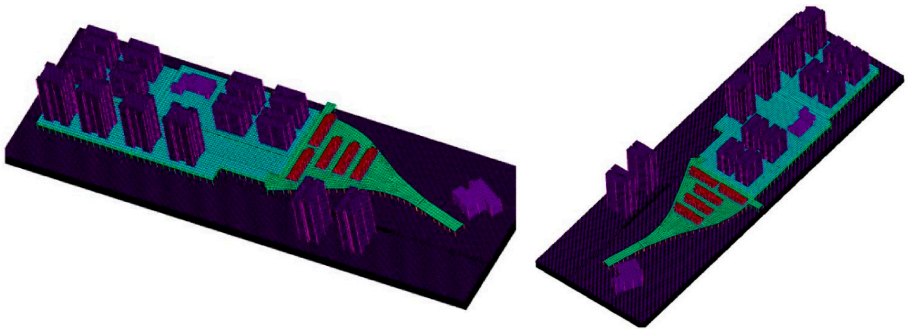


Figure 3. Overall Finite Element Model.

3.2. Model Validation Based on Field Measurements

3.2.1. Field Measurement System and Parameter Settings

To ensure the accuracy and reliability of the test data, a 941B ultra-low-frequency vibration sensor (Institute of Engineering Mechanics, China Earthquake Administration, Beijing, China) was employed in this study for vibration acceleration measurements. This sensor is a piezoelectric seismic sensor. Compared with conventional geophones, which typically have a frequency response range of 1–100 Hz and exhibit a pronounced reduction in sensitivity in the high-frequency range, the adopted sensor provides a frequency response range of 0.25–1000 Hz, thereby fully covering the vibration frequency band of building structures induced by metro operation. The sensor sensitivity is 300 $mV/(m \cdot s^{-2})$, and the measurement range is $\pm 20\ m/s^2$, which satisfies the requirements of low-amplitude and broadband vibration testing for this project. Data acquisition was carried out using an INV3060S 24-bit multi-channel synchronous data acquisition system. The sampling frequency was set to 1024 Hz, and the sampling duration for a single train pass was 30 s. Effective data

were collected using a level-triggered acquisition mode, with the trigger threshold set at 0.005 m/s^2, so as to avoid interference from environmental background noise.

In this study, the upper limit of the analysis frequency band for vibration signals was set to 125 Hz, mainly for the following reasons:

(1) A large number of studies, both domestic and international, have shown that more than 95% of the vibration energy of building structures induced by metro train operation is concentrated in the low-frequency range of 10–125 Hz, with the dominant frequencies mainly distributed within 31.5–63 Hz. The proportion of vibration energy above 125 Hz is generally less than 5%, and its influence on building structures and human comfort can therefore be regarded as negligible.

(2) According to the evaluation standards applicable to this study, namely the Standard for Limits and Measurement Methods of Building Vibration and Structure-Borne Secondary Noise Induced by Urban Rail Transit (JGJ/T 170-2009) and the Standard for Urban Regional Environmental Vibration (GB 10070-1988) [28], the specified vibration evaluation frequency band is 1–80 Hz.

(3) The VC curve method is mainly used for evaluating special buildings that are highly sensitive to microvibration, such as precision instrument facilities and semiconductor manufacturing workshops, and its evaluation upper limit is 80 Hz. In contrast, the present study focuses on the assessment of occupant comfort in civil buildings such as residential, office, and rental buildings. In order to comprehensively capture potentially existing high-frequency vibration components and avoid overlooking possible exceedance frequency bands, the upper limit of the analysis frequency band was moderately extended to 125 Hz.

3.2.2. Layout of Monitoring Points and Model Validation

To ensure the reliability of the simulation results, field vibration measurements were conducted under the operational conditions of the parking yard, and the test results at corresponding monitoring points were compared with the simulation outputs to assess the accuracy of the model calculations. During the tests, trains passed through the throat area at approximately 12 km/h and entered the depot at around 5 km/h. Based on the distribution of buildings and the site zoning, representative locations were selected for monitoring points, as shown in Figure 4. A total of nine monitoring sections were established: Sections 1–6 were symmetrically arranged in Zone B (measuring points 1–3 on one side, measuring points 4–6 on the opposite side), and measuring points 7–9 were located in Zone C, as shown in Figures 5 and 6. For the underground layer, monitoring points were placed at the pile foundations and outside the track bed, while surface points were positioned either above the pile foundations or at structurally weaker locations between piles.

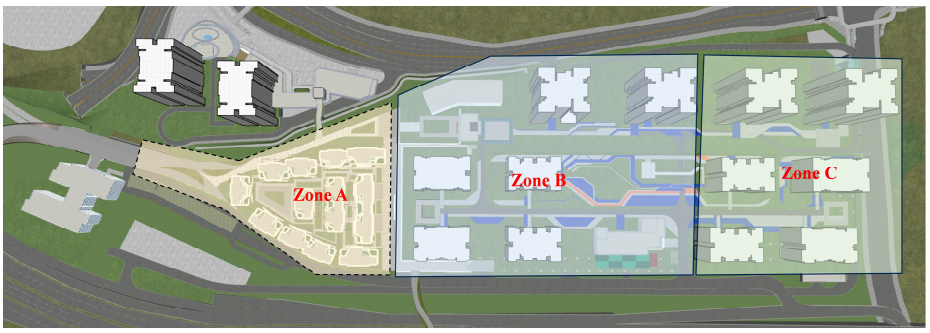


Figure 4. Schematic of Site Zoning.

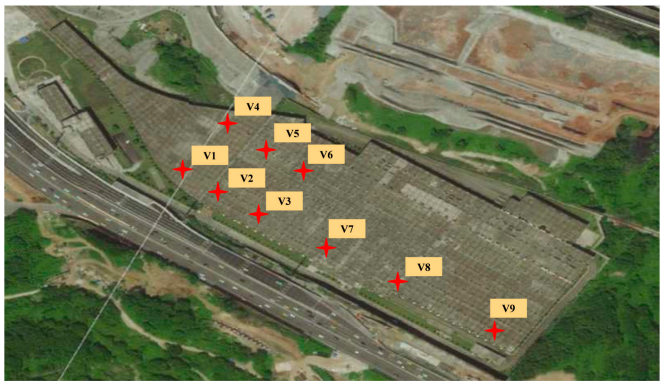


Figure 5. Layout of Monitoring Points.

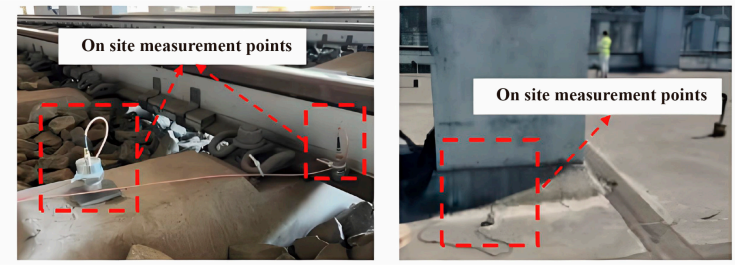


Figure 6. On-site Monitoring.

According to the "Standard for Limits and Measurement Methods of Building Vibration and Structure-Borne Secondary Noise Induced by Urban Rail Transit" (JGJ/T 170-2009), the measured acceleration data were converted into Z-weighted vibration acceleration levels using the prescribed calculation formula. The monitoring results at the V3 and V6 surface points were compared with the corresponding simulation results, as shown in Figures 7 and 8. A summary of the comparison between the measured and calculated results at the remaining monitoring points is provided in Table 4.

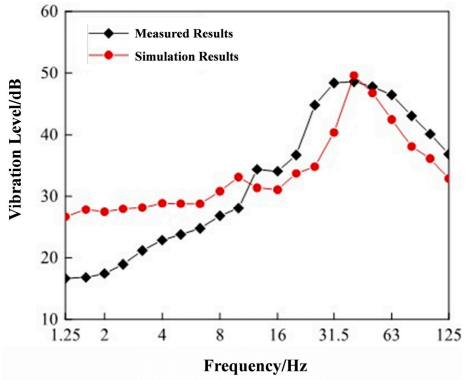


Figure 7. Comparison of Vibration at Monitoring Point V6.

According to the time-domain and frequency-domain comparison plots at measuring points V3 and V6, the simulated and measured acceleration amplitudes are generally in good agreement. However, owing to non-stationary factors during actual train operation, such as stopping, horn sounding, and slight speed fluctuations, local abrupt changes may appear in the measured time–history curves. In contrast, in the simulation, the train operates at a constant prescribed speed, resulting in stronger continuity of the time-domain signals [29]. Although certain differences exist in local peak values and octave-band vibration levels, the dominant vibration frequencies agree well, and the response patterns at

all measuring points are generally consistent. As shown in Table 4, both the vibration level and the peak acceleration at the measuring points above the throat section are significantly higher than those in other areas. This result is consistent with the engineering reality that the turnout throat section of the parking yard is the principal vibration source, thereby verifying the rationality and reliability of the established model. Further analysis of Table 4 shows that the percentage difference in peak acceleration ranges from 0.00% to 12.50%, with an average of 7.21%, while the percentage difference in the maximum Z vibration level ranges from 0.47% to 4.00%, with an average of 2.68%.

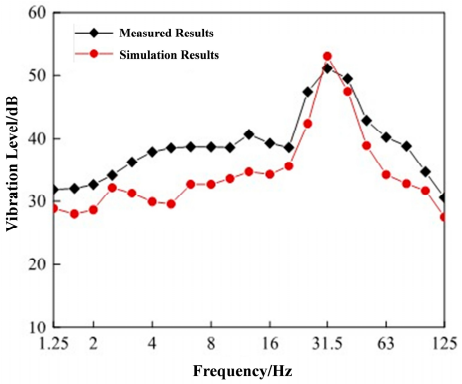


Figure 8. Comparison of Vibration at Monitoring Point V3.

Table 4. Comparison Between Calculated and Measured Results.

Monitoring Point	Peak Acceleration/(m/s^2)		Difference (%)	Maximum Z-Vibration Level/(dB)		Difference (%)
	Measured Result	Calculated Result		Measured Result	Calculated Result	
V1	0.037	0.041	10.81	68.8	70.2	2.03
V2	0.029	0.032	10.34	63.3	63.6	0.47
V3	0.026	0.029	11.54	63.1	65.3	3.49
V4	0.052	0.052	0	67.8	69.5	2.51
V5	0.048	0.049	2.08	60.0	62.4	4.00
V6	0.042	0.044	4.76	58.6	60.7	3.58
V7	0.024	0.026	8.33	60.7	61.9	1.98
V8	0.024	0.027	12.50	60.7	62.3	2.64
V9	0.022	0.023	4.55	59.1	61.1	3.38

Overall, the relative deviation of the maximum Z vibration level is clearly smaller than that of the peak acceleration, indicating that the model has relatively high accuracy in characterizing vibration levels. By comparison, the deviation in peak acceleration is slightly larger, which is mainly attributable to fluctuations in actual train operating conditions, locally intensified excitation in the turnout section, and the high sensitivity of transient peaks to working-condition variations. Nevertheless, these differences remain within an acceptable range, and the model can therefore be regarded as reasonable and reliable.

3.3. Analysis of Vibration Characteristics in Different Functional Zones

The buildings on the project development site and the surrounding existing building clusters are divided into functional zones: residential area, reserved area, rental housing area, and office area. The residential area comprises the planned high-rise Buildings 1–13, the reserved area includes the existing Buildings 14 and 15, the rental housing area contains the existing Building 16, and the office area corresponds to the existing Building 17. The functional zones and the plan locations of the buildings are shown in Figure 9.

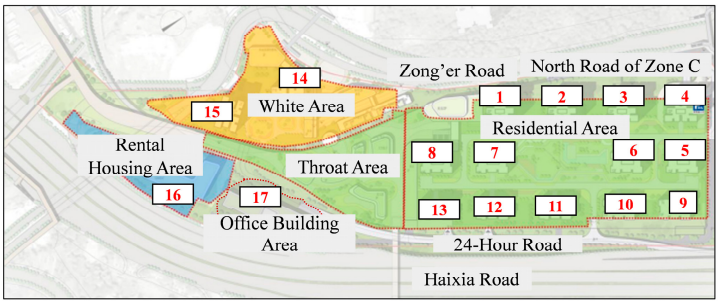


Figure 9. Functional Zone Layout.

According to the "Standard for Environmental Vibration of Urban Areas" (GB 10070-1988) and the "Standard for Limits and Measurement Methods of Building Vibration and Structure-Borne Secondary Noise Induced by Urban Rail Transit" (JGJ/T 170-2009), which specify the frequency-dependent vibration limits and maximum Z-weighted vibration levels for residential buildings, commercial buildings, and basements, and based on the site conditions, this study conducts a vibration characteristics analysis at selected monitoring points.

The vibration monitoring points are located at the floor slab centers of the following levels:

(1) Residential area (Buildings 1–13): 1st, 5th, and 13th floors;
(2) Reserved area (Buildings 14 and 15): 1st, 6th, 11th, 16th, and 21st floors;
(3) Rental housing area (Building 16): 1st, 4th, and 7th floors;
(4) Office area (Building 17): 1st, 4th, and 7th floors.

Figure 10 shows the time-domain vibration results for Buildings 1–13 in the residential area. To more intuitively examine the vibration of each floor within different frequency bands, the time-domain data were further analyzed using one-third octave band analysis, and the resulting frequency-specific vibration levels and maximum Z-weighted vibration levels are summarized in Table 5. The analysis indicates that, for the residential building cluster above the depot, the dominant vibration frequency of the floor slabs induced by the metro is concentrated around 63 Hz. Vibration gradually decays from lower to higher floors, but both the maximum vibration levels and the frequency-specific levels remain within the standard limits. Further analysis shows that Buildings 5–8 exhibit higher peak vibration acceleration and maximum Z-weighted vibration levels compared with adjacent buildings. This is because these buildings are located directly above the track, closer to the vibration source, resulting in more pronounced vibration responses. It is also observed that along the direction of metro movement, the peak vibration accelerations and Z-weighted levels of successive buildings gradually decrease. This is due to the reduction in train speed after passing the throat area, causing the trailing buildings to experience lower vibration levels compared with those closer to the source.

Table 5. Maximum Z-Weighted Vibration Levels and Frequency-Specific Vibration Levels in the Residential Area.

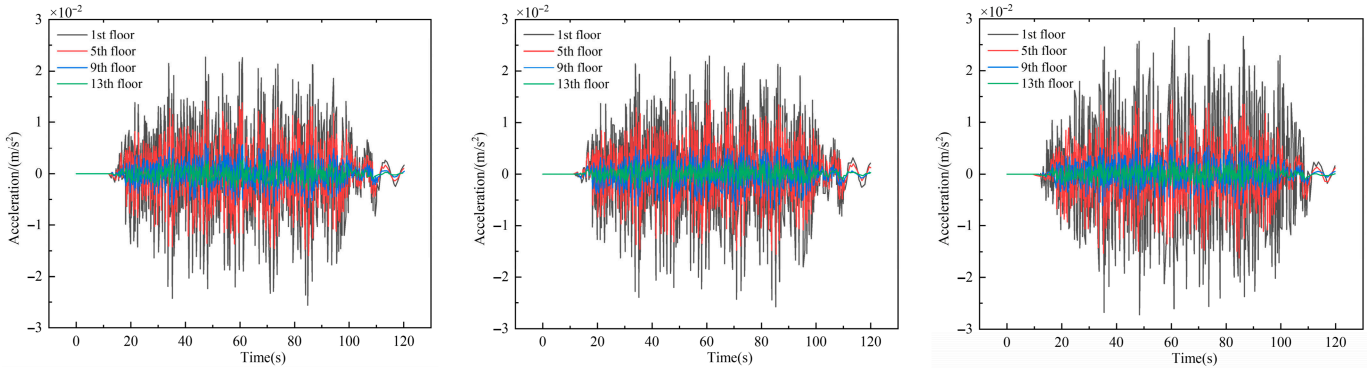
Location		Frequency-Specific Vibration Level	VL_{zmax}
Building 1	1st floor	45.2	47.5
	5th floor	38.2	40.4
	9th floor	35.5	37.2
	13th floor	28.9	31.1

Table 5. *Cont.*

Location		Frequency-Specific Vibration Level	VL_{zmax}
Building 2	1st floor	44.2	46.3
	5th floor	37.3	39.5
	9th floor	36.2	38.2
	13th floor	29.5	32.5
Building 3	1st floor	45.3	47.6
	5th floor	37.9	40.8
	9th floor	35.3	37.6
	13th floor	29.8	32.0
Building 4	1st floor	41.4	43.7
	5th floor	36.2	38.3
	9th floor	30.8	33.5
	13th floor	26.7	29.3
Building 5	1st floor	55.5	47.4
	5th floor	40.9	43.2
	9th floor	37.8	39.3
	13th floor	30.9	33.2
Building 6	1st floor	48.3	50.6
	5th floor	44.2	46.8
	9th floor	39.6	41.9
	13th floor	35.4	37.1
Building 7	1st floor	49.3	51.1
	5th floor	43.7	45.6
	9th floor	38.5	40.8
	13th floor	33.3	35.9
Building 8	1st floor	49.3	51.6
	5th floor	44.1	46.3
	9th floor	36.6	38.8
	13th floor	32.1	34.2
Building 9	1st floor	40.1	42.7
	5th floor	35.2	37.6
	9th floor	31.3	33.6
	13th floor	26.2	28.8
Building 10	1st floor	45.2	47.4
	5th floor	39.7	41.3
	9th floor	34.6	36.6
	13th floor	28.4	30.4
Building 11	1st floor	45.1	48.7
	5th floor	37.2	38.6
	9th floor	33.1	36.1
	13th floor	27.3	29.8

Table 5. *Cont.*

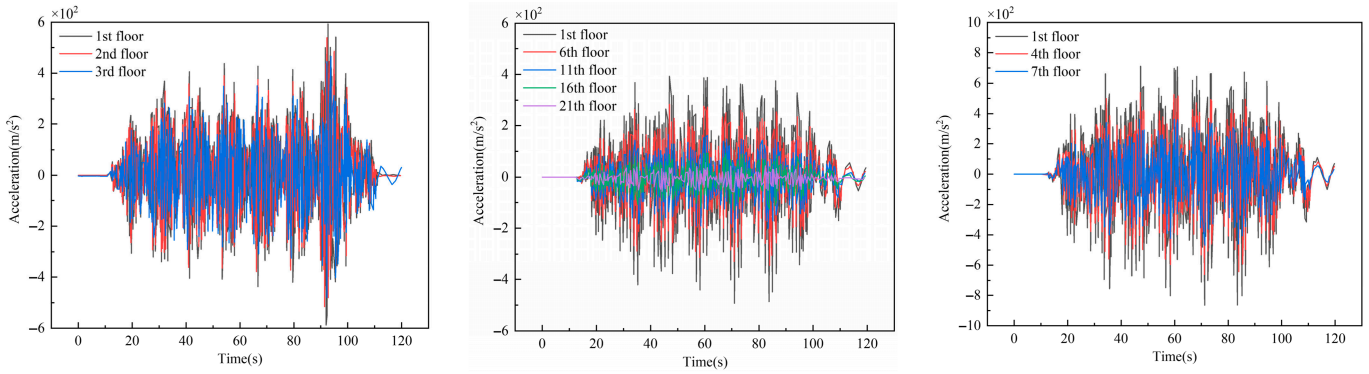
Location		Frequency-Specific Vibration Level	VL_{zmax}
Building 12	1st floor	45.2	47.7
	5th floor	36.3	37.9
	9th floor	32.1	34.1
	13th floor	27.9	29.1
Building 13	1st floor	44.5	46.9
	5th floor	36.8	38.1
	9th floor	32.4	34.5
	13th floor	27.3	29.3



(**a**) (**b**) (**c**)

Figure 10. Time-Domain Vibration Profiles of Each Floor in the Residential Area. (**a**) Vibration domain diagram of each floor of Building 1. (**b**) Vibration domain diagram of each floor of Building 3. (**c**) Vibration domain diagram of each floor of Building 6.

By applying a similar analysis method as used for the residential area, the time-domain vibration results and corresponding vibration levels for the office area buildings, reserved area buildings, and rental housing buildings are summarized in Figure 11 and Table 6, respectively.



(**a**) (**b**) (**c**)

Figure 11. Floor Vibrations of Buildings in Different Functional Zones. (**a**) Vibration of Each Floor in the Office Area Buildings. (**b**) Vibration of Each Floor in the Reserved Area Buildings. (**c**) Vibration of Each Floor in the Rental Housing Area Buildings.

Table 6. Maximum Z-Weighted Vibration Levels and Frequency-Specific Vibration Levels of Residential Area Buildings.

Location		Frequency-Specific Vibration Level	VL_{zmax}
Office Area (Building 17)	1st floor	65.4	67.8
	2nd floor	63.6	66.2
	3rd floor	62.7	65.4
Reserved Area (Building 14)	1st floor	64.4	48.6
	6th floor	60.2	40.2
	11th floor	54.3	36.5
	16th floor	44.6	27.9
	21st floor	32.8	25.7
Reserved Area (Building 15)	1st floor	63.6	46.7
	6th floor	56.8	39.3
	11th floor	53.3	35.8
	16th floor	46.1	27.6
	21st floor	33.3	25.4
Rental Housing Area (Building 16)	1st floor	69.3	70.8
	4th floor	64.8	67.4
	7th floor	59.6	61.3

The analysis indicates that the floor slab vibrations of the office area buildings, reserved area buildings, and rental housing buildings induced by the metro also have dominant frequencies concentrated around 63 Hz, and their vibration characteristics follow the same variation patterns as those observed in the residential area. However, because the reserved area, office area, and rental housing buildings are located closer to the depot throat, and the metro operates at a relatively higher speed when entering the depot, the vibration responses in these zones are greater than those in the residential area. In particular, the 1st floor of Building 16 in the rental housing area exhibits a frequency-specific vibration level of 69.3 dB, approaching the standard limits of 70 dB/67 dB. Although frequency-specific levels at other locations do not exceed the limits, the safety margins are relatively small.

3.4. Analysis of Structure-Borne Secondary Noise Characteristics

Building on the analysis of vibration characteristics, this study further examines the secondary noise characteristics in each functional zone. According to the "Standard for Limits and Measurement Methods of Building Vibration and Structure-Borne Secondary Noise Induced by Urban Rail Transit" (JGJ/T 170-2009), the indoor secondary structure-borne noise limits for buildings along urban rail lines are specified as follows:

(1) Residential buildings are classified under "residential and educational areas", with allowable sound pressure levels of 38/35 dB (daylight/nighttime).
(2) Commercial buildings and basements are classified under "mixed residential-commercial areas and commercial centers", with allowable sound pressure levels of 41/38 dB (daylight/nighttime).

The maximum sound pressure levels of structure-borne secondary noise in each functional zone are summarized in Table 7. It can be observed that, when evaluating the environmental impact induced by train operations, the standards for secondary noise are stricter than those used for vibration assessment. As a result, most monitoring points

show exceedances in secondary noise levels. Specifically, the 1st and 4th floors of the rental housing area exceed the limits, and the office area shows exceedances on the 1st, 2nd, and 3rd floors, with a maximum exceedance of 8.7 dB. Only the reserved area and residential buildings remain within the limits, though with relatively small safety margins. Therefore, based on the combined analysis of vibration characteristics and secondary noise characteristics, it is necessary to implement appropriate vibration mitigation and noise reduction measures to ensure compliance with the relevant standards.

Table 7. Maximum Sound Pressure Levels of Structure-Borne Secondary Noise in Different Functional Zones.

Location		Maximum Sound Pressure Level (dB)
Residential Area	1st floor	37.1
	5th floor	36.8
	9th floor	30
	13th floor	24.1
Office Area	1st Floor	43.7
	2nd Floor	41.5
	3rd Floor	38.3
Reserved Area	1st floor	37.5
	6th floor	31.3
	11th floor	26.6
	16th floor	21.2
	21st floor	19.1
Rental Housing Area	1st floor	46.7
	4th floor	41.3
	7th floor	36.5

3.5. Preceptions Levels

According to the Standard of Environmental Vibration in Urban Areas (GB 10070-1988) and the Standard for Limit and Measuring Method of Building Vibration and Secondary Radiated Noise Caused by Urban Rail Transit (JGJ/T 170-2009), both building vibration and indoor secondary radiated noise can serve as important indicators for evaluating human perception levels. Among them, the maximum Z vibration level can characterize the degree to which floor vibration induced by train operation affects occupants, while the sound pressure level of secondary radiated noise reflects the subjective perceptibility of indoor low-frequency vibration-induced noise. Because the assessment criteria for secondary radiated noise are generally more stringent than those for vibration control, occupants may still perceive environmental disturbance through audible indoor noise even when vibration levels do not obviously exceed the prescribed limits.

As shown in Tables 5 and 6, the maximum Z vibration levels on different floors in the residential area range from 31.1 to 51.6 dB, and those in the daytime-use area range from 25.4 to 48.6 dB, both of which are significantly below the corresponding limit values. This indicates that the vibration induced by train operation in these two types of areas is generally within an acceptable range, with weak human vibration perception and little likelihood of causing noticeable discomfort. In contrast, the maximum Z vibration levels in the office area range from 65.4 to 67.8 dB, while those in the rental area range from 61.3 to 70.8 dB. Among them, the first floor of the rental area has exceeded the limit, and the fourth

floor of the rental area as well as the lower floors of the office area are close to the control threshold. These results indicate that low-rise buildings located near the throat section of the depot are more sensitive to train-induced vibration, leading to a markedly enhanced level of human perceptibility during train passage and a potential risk of reduced comfort at certain locations. Overall, human perception of vibration exhibits a distribution pattern characterized by decreasing intensity with increasing floor height and increasing intensity with decreasing distance to the vibration source.

Further analysis based on Table 7 shows that the secondary structure-borne noise levels in both the residential area and the daytime-use area do not exceed the prescribed limits, indicating that noise disturbance induced by structural vibration in these indoor environments is relatively minor and that the overall subjective perception of occupants remains weak. By contrast, different degrees of exceedance are observed on Floors 1 to 3 of the office area and on Floors 1 and 4 of the rental area, with the maximum exceedance in the office area reaching 8.7 dB. This result suggests that, at these locations, human perception of the environmental impact of rail transit is not limited to floor vibration itself, but is more likely to manifest first as indoor low-frequency rumbling noise or audible structure-borne noise. Therefore, for the lower floors of the office and rental areas, secondary radiated noise is a more sensitive indicator affecting human perception and environmental comfort.

A comprehensive analysis of both vibration and secondary radiated noise results indicates that the human perception level varies significantly across different functional areas of this project. The residential area and the daytime-use area remain generally at a low perception level and can satisfy normal habitation and usage requirements. In contrast, the lower floors of the office and rental areas exhibit relatively high perception levels. In particular, the first floor of the rental area and the lower floors of the office area near the throat section are more likely to cause noticeable vibration and noise perception during train passage, and targeted vibration and noise mitigation measures are therefore required to further improve indoor comfort.

4. Acoustic Environment Evaluation and Noise Propagation Patterns

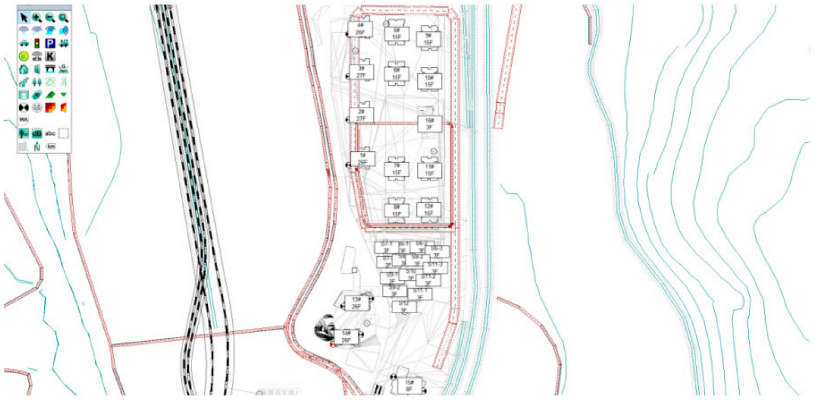
4.1. Establishment of the Acoustic Environment Simulation Model

The project site was modeled at full scale based on the overall site layout, the rail transit Loop Line (depot line), and the metro hub model. During the modeling process, structural components that do not affect the calculation of noise prediction points were simplified. To account for the most adverse conditions, noise prediction points were arranged at the field monitoring locations and 1 m outside the planned buildings, at a height of 1.5 m above each floor level. The plan view and 3D model of the simulation are shown in Figure 12.

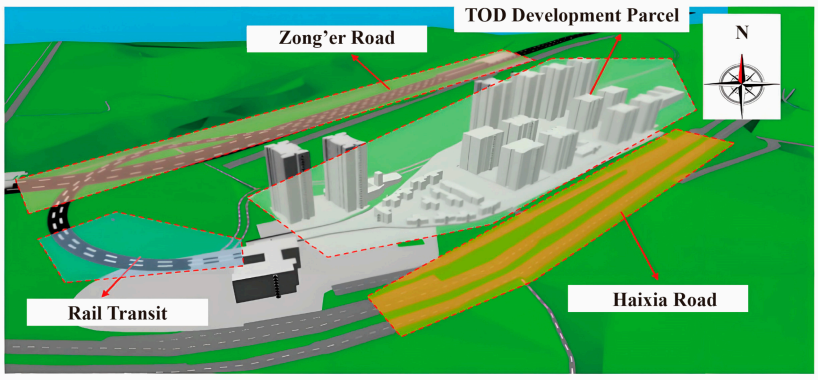
4.2. Model Validation and Correction

4.2.1. Field Measurement System and Parameter Settings for the Acoustic Environment

In this study, environmental noise monitoring was conducted using an AWA6228+ multifunction sound level meter. This instrument meets the Class 1 accuracy requirements specified in Electroacoustics—Sound Level Meters—Part 1: Specifications (GB/T 3785.1-2010). It has a frequency response range of 20 Hz to 12.5 kHz and an A-weighted sound pressure level measurement range of 30 to 130 dB, thereby satisfying the requirements for broadband and high-precision measurement of environmental noise in urban areas. Before and after each measurement, the instrument was calibrated using an AWA6021 acoustic calibrator (Shenzhen Baichuan Electronics Co., Ltd., Shenzhen, China). The calibration sound pressure levels were 94.0 dB (1 kHz) and 114.0 dB (1 kHz), respectively, and the calibration error was controlled within $\pm$0.3 dB to ensure the accuracy of the measurement data.



(**a**) Plan View of the Model



(**b**) Three-dimensional Perspective View of the Model

Figure 12. Schematic Diagram of the Model.

The data acquisition parameters were set as follows. A-frequency weighting and F-time weighting were adopted, with a sampling interval of 1 s, and continuous monitoring was carried out for 24 h to automatically obtain the daytime and nighttime equivalent continuous A-weighted sound levels. During the measurement process, a traffic flow recorder was used simultaneously to collect traffic volume data for Haixia Road and Zong'er Road. The traffic volume was classified and counted by vehicle type, including light, medium, and heavy vehicles. In addition, the number of train operations, operating speeds, and passing times of both the Loop Line and the depot line were recorded. All measurements were conducted under meteorological conditions without rain or snow and with a wind speed not exceeding 5 m/s, so as to eliminate the interference of meteorological factors on the noise measurement results.

4.2.2. Layout of Measurement Points and Model Validation

To calibrate and verify the simulation accuracy of the model, the equivalent sound levels of single-train passages on the Loop Line and the depot line were measured. The results showed that the Loop Line single-train Leq ranged from 81.8 to 82.1 dB, while the depot line single-train Leq was 82.3 dB. Corresponding noise source parameters, including train pass-by sound levels, train speed, and other relevant data, were input into the model and adjusted according to the field measurements. After calibration, the single-train equivalent sound levels at the elevated depot return track monitoring points were determined to be 81.5 dB for the Loop Line and 82.3 dB for the depot line. Once the model was calibrated, nine monitoring points were selected on-site for noise measurement, as shown in Figure 13. Measurements were conducted over a 24 h period, with the daytime defined as 06:00–22:00 and the nighttime as 23:00–05:00 the following day. During

noise monitoring, traffic flow and other relevant information were also recorded [30]. The corresponding points were extracted from the model and compared with the field measurements to validate the accuracy of the acoustic simulation.

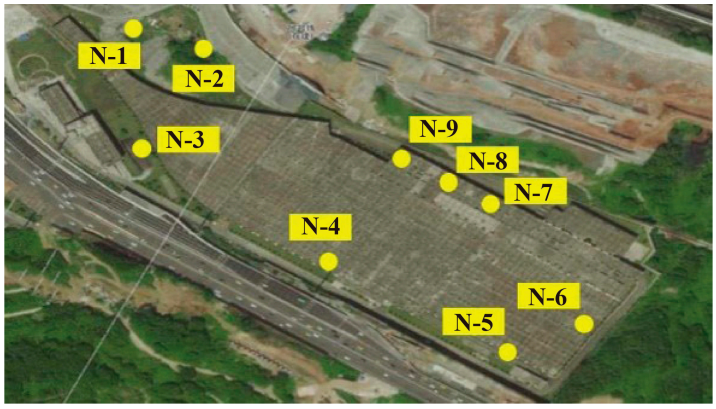


Figure 13. Plan View of Measurement Points.

The field monitoring data at the corresponding points and the model-calculated values are summarized in Table 8. The error is defined as the difference between the measured and simulated values, while the accuracy is calculated as the ratio of the simulated value to the measured value, reflecting the precision of the model. As shown in the table, after calibration, the model exhibits an error of only 0.1–1.1 dB compared with the field measurements, and the simulation accuracy reaches over 98%. This demonstrates that the model can effectively simulate the acoustic environment of the study area, ensuring the reliability of subsequent predictive analyses.

Table 8. Comparison of Actual Monitoring and Simulation Values.

Monitoring Point	Measured Value/dB		Simulated Value/dB		Error/dB		Accuracy/%	
	Daytime	Nighttime	Daytime	Nighttime	Daytime	Nighttime	Daytime	Nighttime
N-1	63.4	62	62.6	61.3	0.8	0.7	98.7%	98.8%
N-2	62.5	60.9	62.2	60.7	0.3	0.2	99.5%	99.6%
N-3	67.1	66.7	65.8	65.6	1.3	1.1	98.1%	98.4%
N-4	64.4	64	64.2	63.4	0.2	0.6	99.6%	99.1%
N-5	61.7	60.3	61.3	60.2	0.4	0.1	99.4%	99.8%
N-6	60.7	59.2	60.4	59.1	0.3	0.1	99.5%	99.8%
N-7	63.4	62.2	62.6	61.1	0.8	1.1	98.7%	98.2%
N-8	63.4	61.7	62.4	60.9	1.0	0.8	98.4%	98.7%
N-9	62.4	61.4	62.4	60.8	0.1	0.6	99.8%	99.0%

4.3. Noise Source Contribution Analysis

The maximum noise contribution values of each building under different conditions were extracted and summarized in Figure 14. From the figure, under road traffic-only conditions, the noise contribution values of Residential Buildings 1–8 show little variation, ranging from 57.6 to 60.3 dB. In contrast, Residential Buildings 9, 10, 11, 12, and 16, which are located closer to the urban arterial Haixia Road, exhibit higher noise levels, ranging from 65.8 to 67.8 dB. The two buildings in the reserved area, Buildings 13 and 14, have noise contributions of 60.9–61.1 dB, similar to Residential Buildings 1–8. The office area S-zone buildings and Rental Housing Building 15 have noise contributions of 64.2 dB and 67.5 dB, respectively. Analyzing the noise contributions under metro-only conditions, it can be observed that the values are related to both the train speed and the planar distance from the train. When the train passes through the throat area, its speed is relatively high, generating

higher noise levels. Consequently, buildings near the throat area—such as the reserved area buildings, rental housing building, office area S-zone buildings, and Residential Buildings 1 and 8—exhibit higher noise contributions, ranging from 55.1 to 62.3 dB. As the train slows down after leaving the throat area, the noise contributions of nearby buildings decrease; this trend is clearly observed in Residential Buildings 5–8, where the noise contribution decreases from 58 dB at Building 8 to 47.2 dB at Building 5. Meanwhile, Buildings 9, 10, 11, 12, and 16, which are farther from the train tracks, show relatively lower noise contributions, ranging from 43.4 to 47.7 dB.

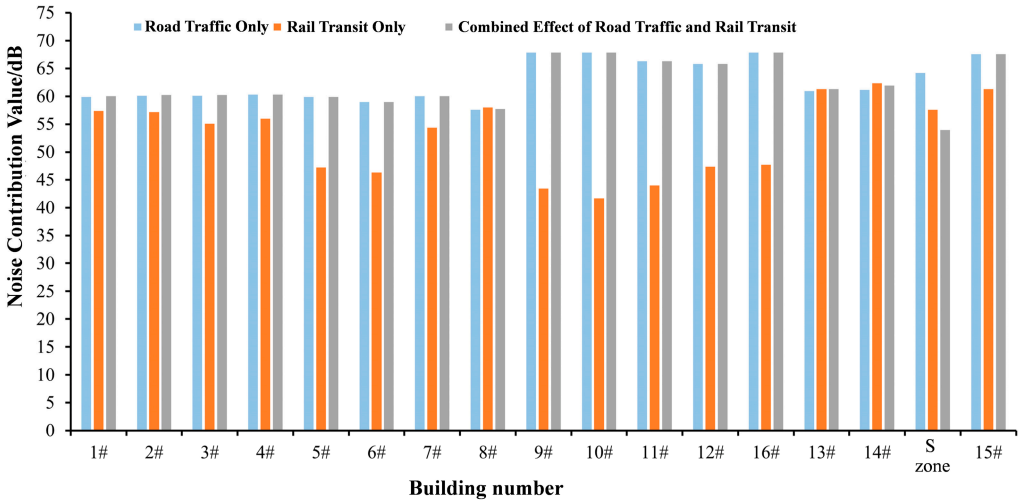
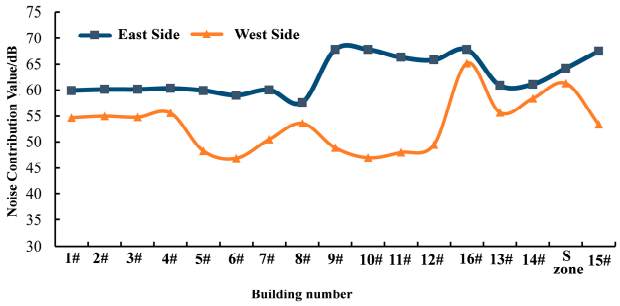


Figure 14. Maximum Noise Contribution Values of Each Building.

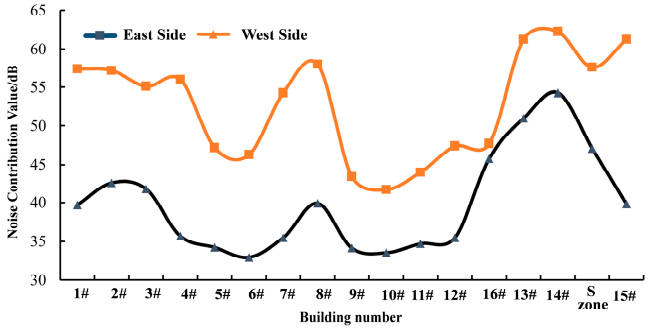
A comparative analysis of the noise contributions under road-only and metro-only conditions shows that the noise levels from road traffic are generally higher than those from metro operations for most buildings. This difference is particularly pronounced for Buildings 9, 10, 11, 12, and 16, which are adjacent to the urban arterial and secondary roads. These roads experience heavy traffic, a large number of vehicles, and high traffic density, whereas metro operations are typically scheduled and more regular, with possible reductions or suspensions during nighttime. Consequently, the per-unit-time noise generated by metro trains is lower than that produced by road traffic. Moreover, during the design and construction of metro systems, noise mitigation and vibration isolation measures are often incorporated to reduce the impact on the surrounding environment. Therefore, in the overall assessment, the road traffic contribution dominates the total noise contribution, accounting for a larger proportion of the overall noise levels.

Considering that the east and west facades of each building floor face different noise sources, this study further identifies the primary noise contributors under different conditions by plotting the east- and west-side noise contributions for each scenario, as shown in Figure 15. The analysis indicates that under road-only conditions, the east-side noise contributions of each floor are consistently higher than those on the west side, with differences ranging from 2.7 dB to 20.8 dB. In contrast, under metro-only conditions, the east-side noise contributions are again higher, with differences ranging from 8 dB to 21.5 dB. The underlying reasons are as follows: under road-only conditions, the east facades face the urban arterial road, while the west facades face the secondary road. Because the arterial road carries heavier traffic and higher vehicle density, it generates greater noise. Under metro-only conditions, the train travel direction is mostly along the east side of the buildings, resulting in higher east-side noise contributions. When road traffic and metro operations are combined, the east-side noise contributions remain higher for most buildings, indicating

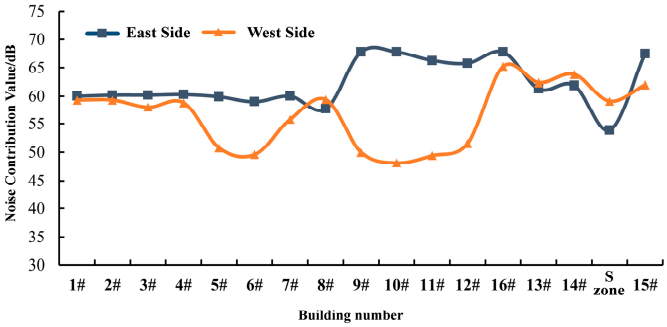
that the road traffic contribution dominates the total noise contribution, which confirms the conclusions drawn earlier.



(**a**) Noise Contribution Values from Road Traffic Only.



(**b**) Noise Contribution Values from Rail Transit Only.



(**c**) Noise Contribution Values Under Combined Effects.

Figure 15. Noise Contribution Values Under Various Conditions.

According to the relevant provisions of the Environmental Quality Standard for Noise (GB 3096-2008), the present study adopts the Class 4a area limits for the prediction and assessment of the outdoor acoustic environment, namely 70 dB (A) during the daytime and 55 dB (A) during the nighttime. Based on these limit requirements, the noise contribution values of most buildings during the daytime remain within the prescribed limits, whereas the corresponding nighttime noise contribution values exceed the allowable limits. For the buildings that do not exceed the limits, the remaining safety margin is relatively small. To further evaluate the reliability of the conclusion regarding nighttime noise exceedance, a brief statistical analysis was conducted on the nighttime prediction results by considering the error between the monitored and simulated nighttime values listed in Table 8. By taking the absolute errors at the nine nighttime monitoring points as an approximate representation of the uncertainty in the nighttime model prediction, the mean absolute error of the nighttime noise prediction was obtained as 0.59 dB, with a standard deviation of 0.39 dB. At the 95% confidence level, the confidence interval of the mean is estimated to be approximately 0.29–0.89 dB. These results indicate that the overall nighttime prediction error of the model is relatively small, and that the width of the confidence interval is less than 1 dB, demonstrating the good statistical stability of the nighttime noise prediction.

As further shown in Figure 16, the noise contribution values of most buildings at night are higher than the limit of 55 dB (A), and the exceedance magnitudes are significantly greater than the uncertainty range mentioned above. Therefore, the nighttime exceedance can be considered statistically significant. Only for a few buildings with predicted values close to the limit should the exceedance judgment be interpreted with caution in light of the associated uncertainty. On this basis, it can be concluded that the nighttime acoustic environment exceedance in this project is not caused by random model error, but rather reflects the actual response characteristics under the combined influence of regional road traffic and rail transit.

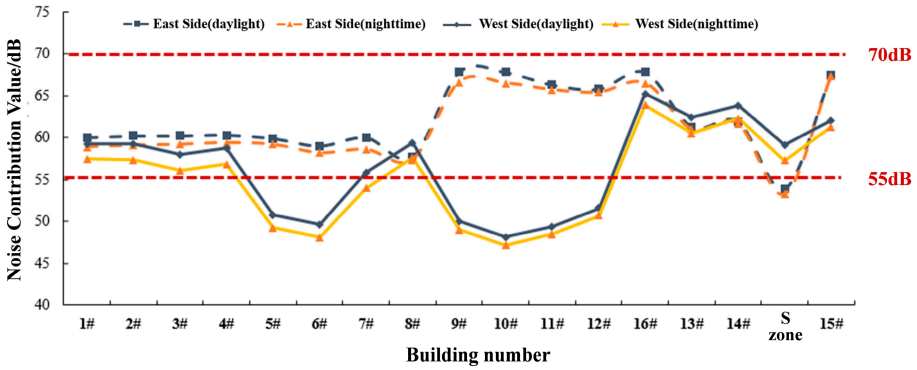


Figure 16. Day and Night Noise Contribution Values of Each Building.

In summary, based on both the comparison with the prescribed limits and the uncertainty analysis of the nighttime prediction results, the nighttime acoustic environment exceedance in this project can be regarded as highly reliable. It is therefore necessary to implement effective noise reduction measures to satisfy the relevant acoustic environment requirements and to ensure the comfort of the living and working environment within the project area.

5. Study on Integrated Vibration and Noise Mitigation Measures

5.1. Principles and Design of Mitigation Measures

The primary principle for vibration and noise mitigation is "source priority and hierarchical control." Source control is the most direct and effective approach. By optimizing the track structure to reduce wheel–rail interaction forces, the input of vibration energy can be minimized at its origin. When source control alone cannot meet the requirements, isolation barriers or sound-absorbing and vibration-damping facilities should be installed along the propagation path to block or attenuate the transmission of vibration waves and sound waves, as shown in Figure 17. For sensitive buildings, protective measures on the receiving structures serve as the last line of defense, further reducing structural vibration responses and indoor noise levels.



(**a**) Vibration-damping fasteners (**b**) Rail seamless welding

Figure 17. Schematic Diagram of Typical Vibration Mitigation Measures.

Based on the above principles and the exceedance characteristics of each functional area in this project, the vibration and noise mitigation measures are determined as follows:

(1) Vibration-damping fasteners are adopted within the residential area. Owing to the large number of buildings and their wide spatial distribution in this zone, the overall vibration levels do not exceed the prescribed limits; however, some buildings located close to the tracks still exhibit relatively pronounced vibration responses, and the overlying track coverage is extensive. Therefore, vibration-damping fasteners are preferentially employed to achieve source control of the wheel–rail interaction excitation, thereby reducing the vibration energy input from the track. This measure does not require modification of the superstructure system and is therefore suitable for large-scale, integrated control of multiple buildings.

For the office area, vibration-isolation supports are installed at the base of the buildings. The vibration and structure-borne secondary noise in the office area are mainly concentrated on the lower floors, indicating that after train-induced vibration enters the superstructure through the foundation, its influence on the indoor environment is more significant in the lower stories. By installing vibration-isolation supports at the building base, the transmission of vibration from the lower structure to the upper floors can be weakened at the entry point of the receiving structure, thereby providing more effective control of floor vibration and the associated secondary radiated noise in the lower floors.

The rental housing area is located close to the throat section of the depot. Under the combined influence of the relatively high train speed during depot entry and the intensified vibration excitation in the turnout zone, the first-floor vibration level and structure-borne secondary noise are the most pronounced, with exceedances mainly concentrated on the side facing the throat section. Therefore, a combined measure consisting of vibration-isolation pads and high-performance vibration-damping fasteners is adopted on this side. The high-performance vibration-damping fasteners are used to further reduce the vibration source intensity of the wheel–rail system, while the vibration-isolation pads are used to locally block the near-field transmission path, thereby mitigating the lateral and vertical propagation of vibration from the track bed and adjacent structures to the over-track buildings. The layout range is shown in Figure 18, and the parameters of the vibration-isolation pads, vibration-damping fasteners, and vibration-isolation supports are listed in Tables 9–11, respectively.

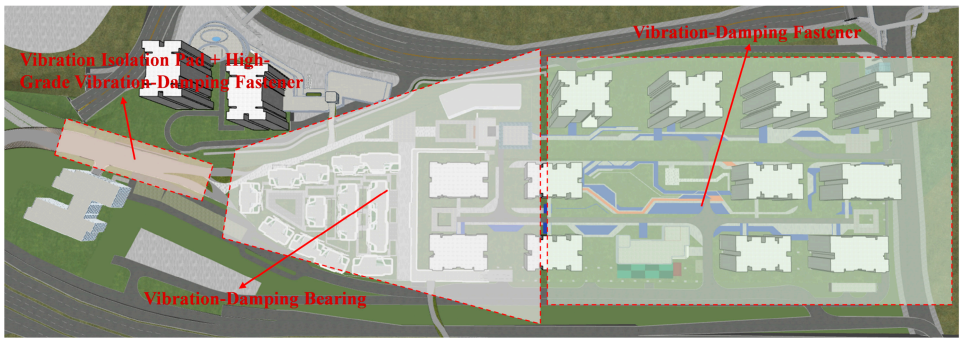


Figure 18. Layout of Vibration Isolation and Mitigation Measures for Each Functional Area.

(2) A 4 m high vertical noise barrier is installed along Haixia Road, and semi-enclosed noise barriers are arranged around the depot line. At the same time, considering that airborne noise from road traffic is the dominant factor in the regional outdoor acoustic environment, and that some buildings may still face a risk of local indoor or outdoor exceedance even after the aforementioned active control measures have been implemented, high-performance sound-insulating windows are further adopted for

the buildings that still exceed the limits in accordance with the indoor noise standard requirements. In this way, an integrated control system combining source vibration reduction, path noise attenuation, and receiver protection is established, as shown in Figure 19.

Table 9. Parameters of Vibration-Isolation Supports.

Structural Parameters	Spring Vibration-Isolation Support
Outer Diameter × Inner Diameter × Thickness × Height/(mm/plate)	500 × 253 × 27 × 38
Elastic Modulus/(kN/mm^2)	206
Poisson's Ratio	0.3
Spring Stiffness/(N/mm)	95,822
Number of Spring Plates	4
Combination Type	Paired Combination

Table 10. Parameters of Vibration-Damping Fasteners.

Structural Parameters	Vibration-Damping Fastener
Rail Type/(kg·m^{-1})	60
Fastener Type	Double-Layer Nonlinear
Fastener Stiffness/(kN·mm^{-1})	15

Table 11. Parameters of Vibration Isolation Pads.

Structural Parameters	Vibration Isolation Pad
Equivalent Stiffness of Isolation Pad/(N/mm^3)	0.01
Thickness/(m)	5



Figure 19. Schematic Diagram of Noise Barriers.

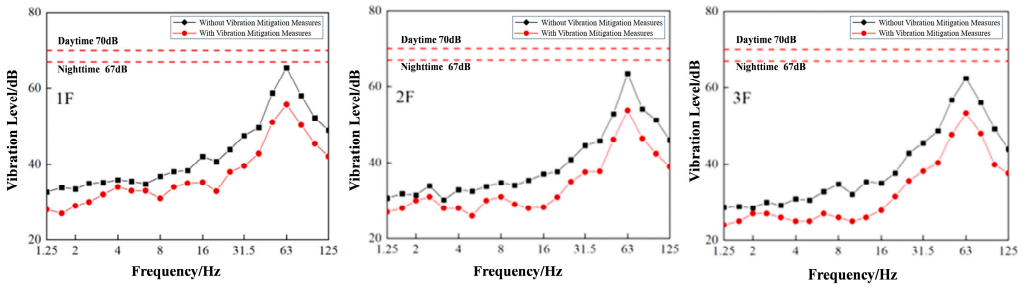
5.2. Analysis of Vibration Mitigation Effectiveness

Based on the vibration mitigation methods and parameters described in the previous section, finite element simulations were conducted for this project, and the vibration and secondary radiation noise of buildings exceeding limits after mitigation were extracted and summarized in Table 12 and Figure 20.

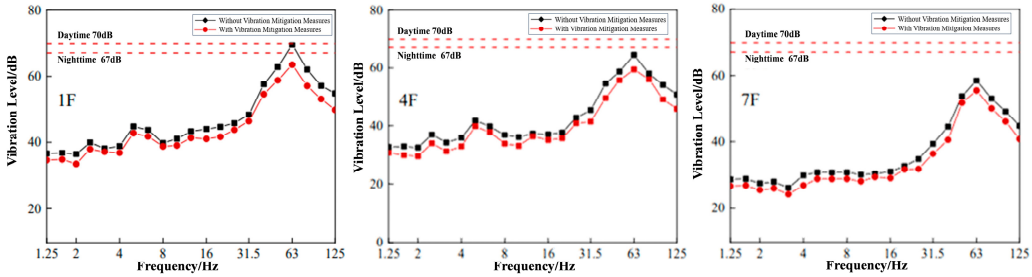
After implementing the corresponding vibration isolation and mitigation measures in each functional area, the vibration and secondary noise at the observation points significantly decreased, with all indicators reduced to within the standard limits. The maximum Z-direction vibration level decreased by 4–8.9 dB, and the maximum sound pressure level decreased by 6.2–9.6 dB, indicating that the vibration isolation and mitigation measures adopted in this project are effective in controlling structural vibration and secondary noise.

Table 12. Vibration Level Analysis of Office and Rental Areas.

Location		Frequency-Weighted Vibration Level	Maximum Vibration Level
Office Area	1st Floor	56.2	58.9
	2nd Floor	55.3	57.5
	3rd Floor	33.7	55.6
Rental Area	1st Floor	64.8	65.3
	4th Floor	58.9	59.6
	7th Floor	53.5	54.7



(**a**) Vibration Attenuation of Office Area Buildings.



(**b**) Vibration Attenuation of Rental Area Buildings.

Figure 20. Comparison of Vibration Characteristics Before and After Mitigation.

5.3. Analysis of Noise Reduction Effectiveness

By implementing active noise reduction measures, such as vertical noise barriers and semi-enclosed noise barriers, the noise contribution values at each monitoring point are summarized in Figure 21. It can be observed that the site's acoustic environment has been significantly improved, with the number of buildings exceeding the limit reduced from 10 to 4, showing a marked decrease. Subsequently, high-performance sound-insulating windows were installed in buildings that still exceeded the limits, thereby ensuring that the daily living and working acoustic environment requirements within the area are met.

Based on the numerical simulation analysis of the aforementioned vibration mitigation and noise reduction measures, the integrated control system adopted in this project demonstrates satisfactory control performance. In terms of vibration control, the combined application of multi-level mitigation measures, including the replacement of conventional fasteners with resilient fasteners, the installation of spring vibration-isolation supports, and the addition of side-wall vibration-isolation pads, effectively suppresses the vibration response in the office and rental housing areas. The frequency-specific vibration levels and the maximum Z-weighted vibration levels at all monitoring points are reduced to within the prescribed limits, with the most pronounced improvement observed on the first floor of the rental housing area, where the exceedance was previously the most severe. The control effect on secondary noise is highly correlated with the attenuation of structural vibration.

As the vibration energy of the floor slabs decreases, the structurally radiated noise correspondingly declines significantly, and the maximum sound pressure levels on all floors in the office and rental housing areas are reduced to within the applicable daytime and nighttime limits for their respective functional zones. Among them, the most remarkable improvement is observed on the first floor of the office area, where the exceedance had originally been the most prominent.

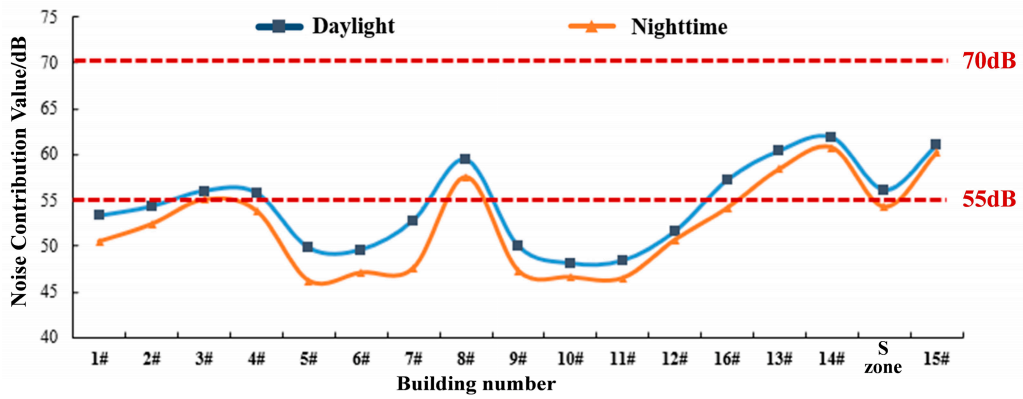


Figure 21. Noise Contribution Values of Each Building After Implementing Noise Reduction Measures.

With regard to the improvement of the acoustic environment, the combined installation of vertical noise barriers and semi-enclosed noise barriers effectively blocks the propagation of airborne noise from both road traffic and rail transit. Together with the supplementary application of high-performance sound-insulating windows, the daytime and nighttime noise contribution values of all buildings within the project area are reduced to meet the requirements of the Class 4a area standard. The nighttime noise reduction effect is particularly significant for several high-rise buildings located close to the arterial road. Further analysis indicates that the acoustic environment problem in this project exhibits a "dual-dominant" characteristic. From the perspective of regional overall sound level control, airborne noise from road traffic is the primary source responsible for the exceedance of the outdoor acoustic environment. In contrast, from the perspective of indoor comfort control, the low-frequency structure-borne noise induced by metro vibration constitutes an important influencing factor for sensitive low-floor spaces in the office and rental housing areas. Therefore, it is difficult for external noise reduction measures alone, such as noise barriers, to effectively mitigate indoor structure-borne secondary noise, while vibration mitigation measures alone are also insufficient to resolve the exceedance of the overall outdoor sound level dominated by road traffic.

Overall, the coordinated implementation of vibration mitigation and noise reduction measures leads to a systematic improvement in both the vibration environment and the acoustic environment within the project area. Among these measures, track vibration reduction and building vibration isolation mainly target metro-induced vibration and the associated low-frequency structure-borne noise, whereas noise barriers and sound-insulating windows are primarily intended to control airborne noise from road traffic and externally radiated noise from rail transit. These two categories of measures correspond to different control requirements associated with distinct propagation mechanisms and spectral characteristics, and together they constitute an integrated mitigation path suitable for TOD over-track development projects. All key evaluation indices satisfy the relevant code requirements, thereby verifying the scientific basis and engineering applicability of the proposed integrated mitigation scheme.

5.4. Cost–Benefit Analysis of Integrated Control Measures

Considering that different control measures vary in terms of implementation scope, construction complexity, maintenance requirements, and control effectiveness, a brief cost–effectiveness analysis is conducted in this study from the perspective of engineering applicability. In general, track vibration mitigation measures act directly on the vibration source or the initial transmission path and therefore usually exhibit relatively high vibration control efficiency, particularly in areas where both structural vibration and structure-borne secondary noise need to be controlled. Building vibration isolation measures are more targeted in their application and are thus suitable for the focused treatment of locally sensitive buildings. Measures aimed at propagation path interruption and receiver protection are more applicable to the control of outdoor acoustic environments dominated by road traffic, as well as to localized supplementary mitigation.

From the perspective of vibration mitigation, vibration-damping fasteners are mainly arranged within the residential area. Their implementation is relatively mature, they have limited impact on the modification of existing track systems, and the investment required per unit coverage is relatively controllable, making them suitable for large-scale application. Their main advantage lies in reducing the vibration input generated by wheel–rail interaction at the source, thus offering good overall cost-effectiveness. Vibration-isolation supports are mainly installed at the base of the office buildings. Although they require relatively higher standards for local structural treatment and installation, they provide a marked control effect on vibration in sensitive low-rise buildings and are therefore suitable for buildings with higher comfort requirements and concentrated exceedances. The combined use of vibration-isolation pads and high-performance vibration-damping fasteners is applied on the side of the rental housing area close to the throat section. This scheme is highly targeted and produces a particularly significant improvement in the area where the original exceedance was most pronounced. However, its implementation scope is relatively concentrated and the structural treatment is more refined, making it a localized high-efficiency mitigation solution. A comprehensive comparison indicates that, for areas where both vibration and secondary noise exceed the limits, priority should be given to a combination of source-level vibration reduction and local building vibration isolation, as this approach can achieve a better balance between control effectiveness and engineering investment.

From the perspective of noise reduction, vertical noise barriers and semi-enclosed noise barriers can significantly attenuate the noise transmitted from road traffic and rail transit to building facades. These measures are suitable for scenarios in which multiple buildings are simultaneously affected and thus provide good group-level control benefits. By contrast, high-performance sound-insulating windows are mainly applied to individual buildings that still approach or exceed the prescribed limits after the implementation of the aforementioned active measures. They serve as supplementary receiver-oriented enhancement measures, with a more concentrated control target and a smaller implementation scope, and are therefore more suitable as terminal optimization measures. In the present project, after the implementation of the active noise reduction measures, the number of buildings exceeding the limits was reduced from 10 to 4, indicating that the noise barrier measures played a dominant role in the overall improvement of the acoustic environment. The sound-insulating windows were then used to further eliminate the remaining exceedance points, thereby ensuring that all buildings complied with the daytime and nighttime limits. This demonstrates that, for TOD projects dominated by road traffic noise and involving a relatively large number of affected buildings, priority should be given to propagation path control measures because of their higher overall benefit, whereas receiver protection measures are more suitable as local supplements. Overall, for areas where

vibration and structure-borne secondary noise are prominent, priority should be given to measures such as vibration-damping fasteners, vibration-isolation supports, and vibration-isolation pads so as to improve the vibration control benefit per unit investment. For areas where nighttime outdoor noise generally exceeds the limits, priority should be given to propagation path interruption measures such as noise barriers so that multiple buildings can benefit simultaneously. For buildings that still exhibit local exceedance after the adoption of the aforementioned measures, the use of high-performance sound-insulating windows as supplementary treatment is more economical and reasonable.

6. Conclusions

This study, taking a Chongqing metro-overlaid TOD project as the engineering background, employs a combination of field measurements and numerical simulations to systematically investigate the vibration characteristics of building clusters induced by metro operation, the propagation patterns of secondary noise, and the spatial distribution of the regional acoustic environment. Targeted comprehensive mitigation measures were proposed and their effectiveness was validated. The main conclusions are as follows:

(1) The vibration response patterns and secondary noise exceedance characteristics of building clusters in different functional zones above the depot under the TOD model were systematically analyzed. The dominant vibration frequency of the floor slabs in all functional zones induced by metro operation is concentrated around 63 Hz, and the vibration response shows a decreasing trend with increasing floor height. A significant vibration amplification effect is observed in the throat area, resulting in the vibration indices on the first floor of the rental housing area, which is closest to this section, exceeding the code limits. The evaluation criteria for secondary noise are more stringent than those for vibration. Exceedances are identified on the 1st to 3rd floors of the office area and on the 1st and 4th floors of the rental housing area, with the maximum exceedance on the first floor of the office area reaching 8.7 dB (A). These results clearly identify the key areas and priority levels for the prevention and control of structure-borne secondary noise in over-track buildings.

(2) The regional acoustic environment is influenced by both road traffic and metro operation, with road traffic being the dominant factor. Under the road-only scenario, buildings 9, 10, 11, 12, and 16 near Haixia Road have noise contributions of 65.8–67.8 dB; under the metro-only scenario, noise contributions are related to train speed and distance from the track, with higher values observed in buildings near the throat section. Noise levels increase with floor height, with the maximum values occurring at the top floors, and east-facing facades generally experience higher noise levels than west-facing ones due to road influence. Daytime noise generally meets Class 4a area standards, while many buildings exceed limits at night.

(3) For vibration control, through the replacement of resilient fasteners, installation of spring isolation bearings, and addition of side-wall isolation pads, the maximum Z-weighted vibration level is reduced by 4–8.9 dB, and the maximum sound pressure level of secondary noise is reduced by 6.2–9.6 dB, bringing all indicators in the office and rental zones within standard limits. Regarding acoustic environment improvement, the combined use of vertical and semi-enclosed noise barriers reduces the number of buildings exceeding limits from 10 to 4, and with the addition of high-performance soundproof windows, noise levels for all buildings during daytime and nighttime comply with Class 4a area standards.

(4) This study addresses the limitation of previous research in which metro-induced vibration and the regional acoustic environment were investigated separately. It achieves the synchronous simulation and combined assessment of coupled

train–track–tunnel–soil–building vibration and regional acoustics, thereby enriching the technical methodology for the integrated evaluation of multi-source vibration and noise in metro over-track TOD projects. The differentiated integrated mitigation scheme proposed in this study provides a feasible solution to engineering problems characterized by substantial differences in vibration and noise control requirements among different functional zones and by the difficulty of quantifying the coordinated effects of multiple mitigation measures. The results can provide a useful reference for environmental impact assessment and refined prevention and control design in similar high-density rail transit over-track development projects.

This study focuses on a metro over-track TOD project in Chongqing, and its conclusions are therefore more applicable to depot over-track development projects with similar site conditions, structural systems, and traffic environments. When extending the findings to other types of projects, project-specific modifications are still required. The evaluation of the integrated mitigation effect is mainly based on numerical models calibrated against field measurements. Although these models can reasonably capture the vibration and noise response characteristics, long-term field data after the implementation of mitigation measures are still needed. In addition, due to the computational limitations of the three-dimensional finite element method in broadband mid- and high-frequency analysis, this study mainly concentrates on low-frequency vibration and the associated secondary noise, while the coupled vibration–noise propagation characteristics over a wider frequency range still require further investigation.

Future research will incorporate comparative analyses of multiple projects under different urban contexts, geological conditions, and overbuild structural forms, so as to further identify the common response characteristics of vibration and acoustic environment in building clusters above metro depots and improve the general applicability of the conclusions. At the same time, long-term operational monitoring data collected after project implementation will be used to continuously calibrate the vibration and acoustic model parameters, with the aim of establishing an integrated analytical framework of "field measurement–simulation–feedback optimization." This will help improve the evaluation accuracy and engineering applicability of comprehensive mitigation measures under long-term operating conditions.

Author Contributions: Data curation, J.L.; formal analysis, J.L.; software, X.X.; project administration, X.X.; funding acquisition, J.W. and W.K.; investigation, J.W., B.Z. and Z.H.; supervision, W.K., B.Z. and Z.H.; resources, Y.M.; writing—original draft, Y.M. and X.K.; writing—review and editing, X.K. All authors have read and agreed to the published version of the manuscript.

Funding: The research described in this paper was financially supported by the National Natural Science Foundation of China (Grant No. 52178302), and the Key R & D Projects in Shaanxi Province (2024SF-YBXM-650).

Data Availability Statement: Data sharing is not applicable to this article as no new data were created or analyzed in this study. No datasets were generated during the current study. All information supporting the reported results can be found within the article.

Conflicts of Interest: Jian Li, Xiaohong Xue, Jian Wang, Wanliang Kang, Boyang Zhang, Zhengye Huang, were employed by the China Railway 20th Bureau Group Sixth Engineering Co., Ltd. The remaining authors declare that the research was conducted in the absence of any commercial or financial relationships that could be construed as a potential conflict of interest.

References

1. Ali, L.; Nawaz, A.; Iqbal, S.; Basheer, M.A.; Hameed, J.; Albasher, G.; Shah, S.A.R.; Bai, Y. Dynamics of Transit Oriented Development, Role of Greenhouse Gases and Urban Environment: A Study for Management and Policy. *Sustainability* **2021**, *13*, 2536. [CrossRef]
2. Wang, J.; Tan, W.; Huang, J. Extending TOD through the Interrelationship between Transport and Land Use: A Case Study of Beijing. *Land Use Policy* **2024**, *144*, 107257. [CrossRef]
3. Zhou, D.; Mei, Y.; Ke, X.; Liu, Z.; Xu, W. Study on the Structural Behavior and Reinforcement Design of Openings in Subway Station Floor Slabs. *J. Build. Eng.* **2024**, *98*, 110994. [CrossRef]
4. Mazzetto, S.; Furlan, R.; Awwaad, R. Sustainable Urban Renewal: Planning Transit-Oriented Development (TOD) in Riyadh. *Sustainability* **2025**, *17*, 4310. [CrossRef]
5. Vos, K.; Peng, Z.; Jenkins, C.; Shahriar, M.R.; Borghesani, P.; Wang, W. Vibration-Based Anomaly Detection Using LSTM/SVM Approaches. *Mech. Syst. Signal Process.* **2022**, *169*, 108752. [CrossRef]
6. Norén-Cosgriff, K.M.; Ramstad, N.; Neby, A.; Madshus, C. Building Damage Due to Vibration from Rock Blasting. *Soil Dyn. Earthq. Eng.* **2020**, *138*, 106331. [CrossRef]
7. Wang, X.; Wang, B.; Yuan, Y.; Yang, T.; Dong, G.; Shi, C. Study on the Effect of EICP Combined with Nano-SiO_2 and Soil Stabilizer on Improving Loess Surface Strength. *Buildings* **2025**, *15*, 1998. [CrossRef]
8. Rauber, T.W.; da Silva Loca, A.L.; Boldt, F.d.A.; Rodrigues, A.L.; Varejão, F.M. An Experimental Methodology to Evaluate Machine Learning Methods for Fault Diagnosis Based on Vibration Signals. *Expert Syst. Appl.* **2021**, *167*, 114022. [CrossRef]
9. Ma, K.W.; Mak, C.M.; Wong, H.M. Effects of Environmental Sound Quality on Soundscape Preference in a Public Urban Space. *Appl. Acoust.* **2021**, *171*, 107570. [CrossRef]
10. Karimi, H.; Adibhesami, M.A.; Bazazzadeh, H.; Movafagh, S. Green Buildings: Human-Centered and Energy Efficiency Optimization Strategies. *Energies* **2023**, *16*, 3681. [CrossRef]
11. Maljaee, S.S.; Khadem Sameni, M.; Ahmadi, M. Effects of Railway Noise and Vibrations on Dissatisfaction of Residents: Case Study of Iran. *Environ. Dev. Sustain.* **2024**, *26*, 2655–2685. [CrossRef] [PubMed]
12. Zar, A.; Hussain, Z.; Akbar, M.; Rabczuk, T.; Lin, Z.; Li, S.; Ahmed, B. Towards Vibration-Based Damage Detection of Civil Engineering Structures: Overview, Challenges, and Future Prospects. *Int. J. Mech. Mater. Des.* **2024**, *20*, 591–662. [CrossRef]
13. Kedia, N.K.; Kumar, A.; Singh, Y. Effect of Rail Irregularities and Rail Pad on Track Vibration and Noise. *KSCE J. Civ. Eng.* **2021**, *25*, 1341–1352. [CrossRef]
14. Scislo, L. Source Based Measurements and Monitoring of Ground Motion Conditions during Civil Engineering Works for High Luminosity Upgrade of the LHC. In Proceedings of the 26th International Congress on Sound and Vibration, ICSV 2019, Montreal, QC, Canada, 7–11 July 2019.
15. Guinchard, M.; Cabon, M.; Charrondière, C.; Develle, K.; Fessia, P.; Lacny, L.L.; Osborne, J.A.; Scislo, L.S.; Wenninger, J. *Investigation and Estimation of the LHC Magnet Vibrations Induced by HL-LHC Civil Engineering Activities, Vancouver, BC, Canada*; JACoW Publishing: Geneva, Switzerland, 2018. [CrossRef]
16. Jing, L.; Wang, K.; Zhai, W. Impact Vibration Behavior of Railway Vehicles: A State-of-the-Art Overview. *Acta Mech. Sin.* **2021**, *37*, 1193–1221. [CrossRef]
17. Thompson, D.J.; Kouroussis, G.; Ntotsios, E. Modelling, Simulation and Evaluation of Ground Vibration Caused by Rail Vehicles*. *Veh. Syst. Dyn.* **2019**, *57*, 936–983. [CrossRef]
18. Ma, S.; Gao, L.; Liu, X.; Lin, J. Deep Learning for Track Quality Evaluation of High-Speed Railway Based on Vehicle-Body Vibration Prediction. *IEEE Access* **2019**, *7*, 185099–185107. [CrossRef]
19. Mai, R.; Ibrahim, I.S.; Padil, K.H.; Sarbini, N.N.; Fu, H.; Chiew, S.M.; Jiang, S. Vehicle Induced Vibration Analysis on Floor Building: A State of the a Rt Review. *J. Vib. Eng. Technol.* **2025**, *13*, 520. [CrossRef]
20. He, W.; He, K.; Zou, C.; Yu, Y. Experimental Noise and Vibration Characteristics of Elevated Urban Rail Transit Considering the Effect of Track Structures and Noise Barriers. *Environ. Sci. Pollut. Res.* **2021**, *28*, 45903–45919. [CrossRef]
21. Khan, D.; Burdzik, R. Measurement and Analysis of Transport Noise and Vibration: A Review of Techniques, Case Studies, and Future Directions. *Measurement* **2023**, *220*, 113354. [CrossRef]
22. Nielsen, J.C.O.; Pieringer, A.; Thompson, D.J.; Torstensson, P.T. Wheel–Rail Impact Loads, Noise and Vibration: A Review of Excitation Mechanisms, Prediction Methods and Mitigation Measures. In *Proceedings of the Noise and Vibration Mitigation for Rail Transportation Systems*; Degrande, G., Lombaert, G., Anderson, D., de Vos, P., Gautier, P.-E., Iida, M., Nelson, J.T., Nielsen, J.C.O., Thompson, D.J., Tielkes, T., et al., Eds.; Springer International Publishing: Cham, Switzerland, 2021; pp. 3–40.
23. Masri, J.; Amer, M.; Salman, S.; Ismail, M.; Elsisi, M. A Survey of Modern Vehicle Noise, Vibration, and Harshness: A State-of-the-Art. *Ain Shams Eng. J.* **2024**, *15*, 102957. [CrossRef]
24. Rui, J.; Lin, W.; Pei, L. Summary of Research on Supporting Facilities and Structure Vibration and Noise Reduction of High-Rise Buildings. *IOP Conf. Ser. Earth Environ. Sci.* **2021**, *791*, 12023. [CrossRef]

25. China Architecture Publishing & Media Co., Ltd. *Standard for Limit and Measuring Method of Building Vibration and Secondary Noise Caused by Urban Rail Transit*; China Architecture Publishing & Media Co., Ltd.: Beijing, China, 2009.
26. Auersch, L. Simple and Fast Prediction of Train-Induced Track Forces, Ground and Building Vibrations. *Railw. Eng. Sci.* **2020**, *28*, 232–250. [CrossRef]
27. Demir Sahin, D.; Eker, H. Environmental Assessment of Blasting in a Copper Quarry. *Sylwan* **2025**, *38*, 62–98. [CrossRef]
28. Qu, S.; Yang, J.; Zhu, S.; Zhai, W.; Kouroussis, G.; Zhang, Q. Experimental Study on Ground Vibration Induced by Double-Line Subway Trains and Road Traffic. *Transp. Geotech.* **2021**, *29*, 100564. [CrossRef]
29. Wang, T.; He, W.; Wang, D.; Chen, J. Field Measurement and Numerical Simulation of Sound Insulation Characteristics of Buildings along Elevated Urban Rail Lines. *Buildings* **2024**, *14*, 3799. [CrossRef]
30. Song, X.D.; Li, Q.; Wu, D.J. Investigation of Rail Noise and Bridge Noise Using a Combined 3D Dynamic Model and 2.5D Acoustic Model. *Appl. Acoust.* **2016**, *109*, 5–17. [CrossRef]

Disclaimer/Publisher's Note: The statements, opinions and data contained in all publications are solely those of the individual author(s) and contributor(s) and not of MDPI and/or the editor(s). MDPI and/or the editor(s) disclaim responsibility for any injury to people or property resulting from any ideas, methods, instructions or products referred to in the content.